SCIENCE CHINA
Information Sciences

• RESEARCH PAPER •
Special Issue

August 2012 Vol. 55 No. 8: 1816–1829
doi: 10.1007/s11432-012-4630-7

Spotlight SAR sparse sampling and imaging method based on compressive sensing

XU HuaPing[1], YOU YaNan[1]*, LI ChunSheng[1] & ZHANG LvQian[2]

[1]*School of Electronics and Information Engineering, Beihang University, Beijing* 100191*, China;*
[2]*Chinese Academy of Engineering, Beijing* 100088*, China*

Received March 5, 2012; accepted May 5, 2012

Abstract Spotlight synthetic aperture radar (SAR) emits a chirp signal and the echo bandwidth can be reduced through dechirp processing, where the A/D sampling rate decreases accordingly at the receiver. Compressive sensing allows the compressible signal to be reconstructed with a high probability using only a few samples by solving a linear program problem. This paper presents a novel signal sampling and imaging method for application to spotlight SAR based on compressive sensing. The signal is randomly sampled after dechirp processing to form a low-dimensional sample set, and the dechirp basis is imported to reconstruct the dechirp signal. Matching pursuit (MP) is used as a reconstruction algorithm. The reconstructed signal uses polar format algorithm (PFA) for imaging. Although our novel mechanism increases the system complexity to an extent, the data storage requirements can be compressed considerably. Several simulations verify the feasibility and accuracy of spotlight SAR signal processing via compressive sensing, and the method still obtains acceptable imaging results with 10% of the original echo data.

Keywords spotlight SAR, dechirp processing, compressive sensing, radar signal processing

Citation Xu H P, You Y N, Li C S, et al. Spotlight SAR sparse sampling and imaging method based on compressive sensing. Sci China Inf Sci, 2012, 55: 1816–1829, doi: 10.1007/s11432-012-4630-7

1 Introduction

Spotlight mode [1], an operating mechanism of synthetic aperture radar (SAR), is often applied to observe a specific area with a high along-track (azimuth) resolution. This mode continues to illuminate the same area, which is limited in both range and azimuth direction, by steering the antenna, as shown in Figure 1. In this case, the time of illumination for each target is evidently increased, and the synthetic aperture length increases correspondingly, and thus the spotlight mode provides a significant amelioration of the azimuth resolution. To achieve a similar range resolution, chirp signals with large bandwidths are used, which generates a huge amount of data according to the Nyquist sampling theorem. Obviously, real-time supervision of several hotspots can be achieved using the spotlight mode, but the great abundance of data created by multiple area supervision is inconvenient for real-time processing. The storage, transmission and processing of this huge amount of data is thus the main challenge of spotlight SAR system design, and it is difficult to satisfy the exploration requirements.

*Corresponding author (email: youyanan201@ee.buaa.edu.cn)

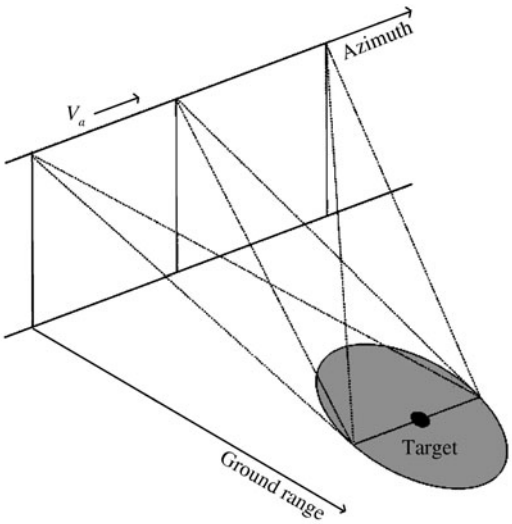

Figure 1 Spotlight SAR acquisition geometry.

Compressive sensing is a dissimilar signal sampling and reconstruction method derived from the traditional Nyquist sampling theorem, and some non-objective conclusions in compressive sensing theory are rooted in the functional analysis and approximation theory [2] established by Kashin. Compressive sensing indicates that a compressible signal under a sparse basis is measured through linear projection into a low-dimensional vector space using a measurement matrix, which is irrelevant with the sparse basis. An original signal is reconstructed with high probability from a few samples through solving a convex optimization problem. The sampling rate is not restricted by the signal bandwidth in compressive sensing, and the signal sampling and storage of the novel method costs much less than that of the Nyquist sampling-based method. If we can detect the appropriate sparse basis, then any signal can be reconstructed with high probability using only a few samples according to compressive sensing principles.

In [3], Baraniuk and Steeghs used the compressive sensing method to process the radar signal, and showed that the receiver system complexity can be reduced by using compressive sensing. Herman and Strohmer designed a high-resolution radar system based on compressive sensing in [4], and they focused on the compressible signal format design. Tello Alonso et al. [5] proposed a two-dimensional SAR imaging approach and Ender [6] summarized several compressive sensing radar systems, but recent research into these compressive sensing radar systems apparently remains deficient, and thus radar systems based on compressive sensing still require an in-depth analysis. In this paper, compressive sensing is applied to spotlight SAR, and we use dechirp processing to construct the sparse basis of the spotlight SAR echoes, finally a suitable data acquisition and processing mechanism is also developed in our research.

The next section briefly introduces and discusses dechirp processing in the spotlight SAR system. In Section 3, we describe the compressive sensing method, and a novel mechanism for data acquisition and processing based on compressive sensing is proposed in this section. Based on the research in the previous sections, simulation results are shown in Section 4, and our final conclusions are presented in Section 5.

2 Dechirp processing in spotlight SAR

SAR often uses the spotlight mode to observe small specific areas precisely. As shown in Figure 1, the direction of the spotlight SAR antenna is controlled with the movement of the radar platform, therefore the exposure time of observed scene is correspondingly improved, i.e., by extending the coherent integration time, and the spotlight mode then obtains a higher azimuth resolution than the stripmap mode. To achieve a high range resolution, spotlight SAR transmits a large bandwidth chirp signal, and the sampling rate of the receiver is at least equivalent to the complex signal bandwidth. The huge amount of data generated by sampling is still the challenge of processing. Range dechirp processing [7–9] can

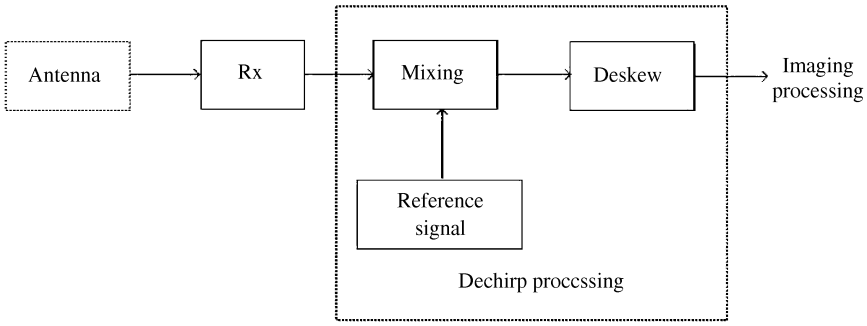

Figure 2 Echo dechirp processing.

compress the spotlight SAR echo bandwidth, and it effectively reduces the system sampling rate.

Assuming that the distance between the scattering center and the radar platform is R, and the target echo received by radar system at a certain azimuth direction is

$$S_r(t) = A\mathrm{rect}\left(\frac{t-2R/c}{T}\right)\mathrm{e}^{\mathrm{j}2\pi f_c(t-2R/c)}\mathrm{e}^{\mathrm{j}\pi K_r(t-2R/c)^2}, \tag{1}$$

where A is the backscatter coefficient of the target, T is the chirp pulse duration time, K_r is the frequency modulation (FM) rate, and f_c is the carrier frequency. The power of the original echo is increased to the designed level by the Rx module, and it is then mixed with the reference signal by different frequency processing, where the reference signal has a fixed time period and the same FM rate as the original echo. Figure 2 shows the dechirp processing of the receiver.

We construct the reference signal as follows:

$$S_{\mathrm{ref}}(t) = \mathrm{e}^{\mathrm{j}2\pi f_c(t-2R_{\mathrm{ref}}/c)}\mathrm{e}^{\mathrm{j}\pi K_r(t-2R_{\mathrm{ref}}/c)^2}, \tag{2}$$

where R_{ref} is the distance between the reference target and the radar platform. By mixing the original echo with the reference signal, the representation is given by

$$S_r(t)\cdot S^*_{\mathrm{ref}}(t) = A\mathrm{rect}\left(\frac{t-2R/c}{T}\right)\mathrm{e}^{-\mathrm{j}\frac{4\pi}{c}[f_c+K_r(t-2R_{\mathrm{ref}}/c)](R-R_{\mathrm{ref}})}\mathrm{e}^{\mathrm{j}\frac{4\pi K_r}{c^2}(R-R_{\mathrm{ref}})^2}. \tag{3}$$

According to Eq. (3), the frequency of the mixing signal is calculated as

$$f_{\mathrm{IF}} = \frac{1}{2\pi}\frac{d\left\{-\frac{4\pi}{c}[f_c+K_r(t-2R_{\mathrm{ref}}/c)](R-R_{\mathrm{ref}})\right\}}{dt} = -\frac{2K_r}{c}(R-R_{\mathrm{ref}}), \tag{4}$$

and then the intermediate frequency signal is

$$S_{\mathrm{IF}}(t) = A\mathrm{rect}\left(\frac{t-2R/c}{T}\right)\mathrm{e}^{\mathrm{j}2\pi f_{\mathrm{IF}}\left(\frac{f_c}{K_r}+t-\frac{2R_{\mathrm{ref}}}{c}\right)}\mathrm{e}^{\mathrm{j}\pi\frac{f_{\mathrm{IF}}^2}{K_r}}. \tag{5}$$

The second exponent term in Eq. (5) is the residual video phase (RVP) produced by dechirp processing, consequently, due to RVP, the echoes of different targets are displaced by their respective time delays. We must compensate for RVP in the frequency domain to achieve deskewed processing. Finally, the echoes of different targets are aligned in the range direction, the expression for the echo is

$$S_{\mathrm{IF}}(t) = A\mathrm{rect}\left(\frac{t-2R/c}{T}\right)\mathrm{e}^{\mathrm{j}2\pi f_{\mathrm{IF}}\left(\frac{f_c}{K_r}+t-\frac{2R_{\mathrm{ref}}}{c}\right)}, \tag{6}$$

and when $t' = f_c/K_r + t - 2R_{\mathrm{ref}}/c$, we rewrite Eq. (6) as

$$S_{\mathrm{IF}}(t') = A\mathrm{rect}\left(\frac{t'-f_c/K_r-2(R-R_{\mathrm{ref}})/c}{T}\right)\mathrm{e}^{\mathrm{j}2\pi f_{\mathrm{IF}}t'}. \tag{7}$$

If we divide the observation scene into N points, where the distance between each discrete point and the radar platform is R_k, and the value of k is an integer from 1 to N, therefore Eq. (4) can be rewritten as

$$f_k = \frac{1}{2\pi}\frac{d\left\{-\frac{4\pi}{c}[f_c + K_r(t - 2R_{\text{ref}}/c)](R_k - R_{\text{ref}})\right\}}{dt} = -\frac{2K_r}{c}(R_k - R_{\text{ref}}), \tag{8}$$

where the expression for the multi-target echoes is

$$S_{\text{IF}}(t') = \sum_{k=1}^{K} A_k \text{rect}\left(\frac{t' - f_c/K_r - 2(R_k - R_{\text{ref}})/c}{T}\right)\text{e}^{\text{j}2\pi f_{\text{IF}}t'}. \tag{9}$$

Obviously, the echoes through dechirp processing are a linear combination of the backscatters on a rectangular window exponent basis.

3 Data acquisition and processing via compressive sensing

3.1 Compressive sensing method

The matrix expression for compressive sensing [10,11] is

$$\boldsymbol{y} = \boldsymbol{\Phi S} = \boldsymbol{\Phi\Psi x}, \tag{10}$$

where $\boldsymbol{S}_{N\times 1}$ is the original signal, $\boldsymbol{\Psi}_{N\times N}$ is the sparse basis of $\boldsymbol{S}_{N\times 1}$, i.e. the sparse representation of $\boldsymbol{S}_{N\times 1}$, and the sparse coefficient is $\boldsymbol{x}_{N\times 1}$. $\boldsymbol{y}_{M\times 1}$ is the measurement vector through a linear projection from the compressible $\boldsymbol{S}_{N\times 1}$. $\boldsymbol{\Phi}_{M\times N}$ (where $M \ll N$) is the projection matrix. Therefore the length of original signal can be reduced by $\boldsymbol{\Phi}_{M\times N}$, and we can use a few measurements to reconstruct the original signal with a high probability.

The restricted isometry property (RIP) [12] is a significant consequence to ensure the convergence of the reconstruction algorithm, and a detailed expression is given for it as follows:

$$1 - \varepsilon \leqslant \frac{\|\boldsymbol{\Phi\Psi x}\|_2}{\|\boldsymbol{x}\|_2} \leqslant 1 + \varepsilon, \quad (\varepsilon > 0), \tag{11}$$

where $||\cdot||_2$ is the l_2 norm, and $\boldsymbol{x}$ is the sparse coefficient vector. The minimization of the l_0 problem shown in Eq. (10) is equivalent to the l_1 norm convex problem under the RIP condition, the irrelevant term between $\boldsymbol{\Phi}_{M\times N}$ and $\boldsymbol{\Psi}_{N\times N}$, for instance, using a Gaussian random matrix as the measurement matrix $\boldsymbol{\Phi}$, almost generally satisfied the RIP with high probability. There are several algorithms available at present to solve this convex problem, with the basis pursuit (BP) being the widely applied algorithm, such as the interior point approach, and the gradient projection method. However, the low efficiency of the calculation restricts the BP algorithm to be employed in real-time re-establishing processing. The greedy pursuit [13–15] gradually becomes the preferential settlement, and then matching pursuit [16] (MP) and orthogonal matching pursuit [17] (OMP) are generally used to recover the original signal.

3.2 Data processing based on the dechirp basis

When comparing Eq. (10) with (9), the echoes S after dechirp processing have a sparse representation $\{A_k\}_{k=1}^{K}$ on the sparse basis, where the expression of the sparse basis is

$$\boldsymbol{\Psi} = \left\{\text{rect}\left(\frac{t' - f_c/K_r - 2(R_k - R_{\text{ref}})/c}{T}\right)\text{e}^{\text{j}2\pi f_k t'}\right\}_{k=1}^{K}, \tag{12}$$

where K is the sparse level, i.e. the number of scatter points in the observed scene. We call this sparse basis the dechirp basis, evidently, the echoes are compressible after dechirp processing, and in each azimuth direction, the echoes can be formatted as a linear combination on the dechirp basis. Considering the characteristics of the dechirp basis, we import dechirp processing based on compressive sensing into a spotlight SAR receiver. The novel receiver is required to randomly collect the original signal during sampling and quantification, therefore the complexity of the data memory and the processing required is decreased. An ameliorative spotlight SAR receiver is shown in Figure 3.

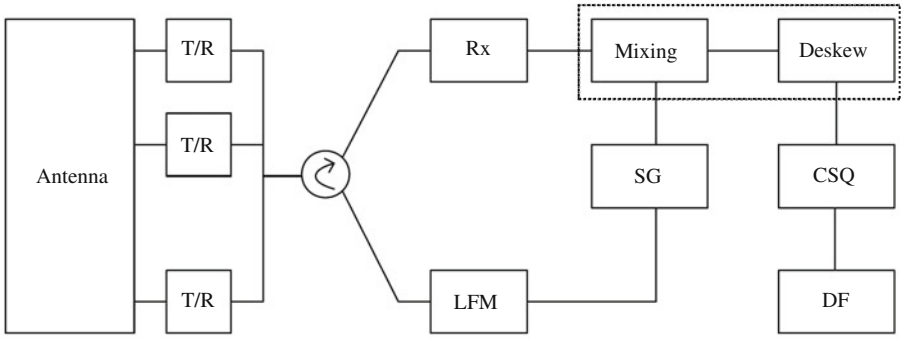

Figure 3 Spotlight SAR receiver based on compressive sensing.

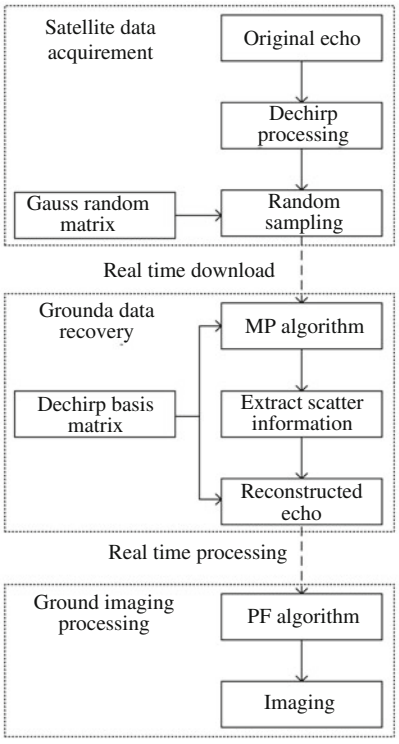

Figure 4 Real-time data acquisition and processing of spotlight SAR based on compressive sensing.

Firstly, the power of the echoes is amplified to the appropriate level by the Rx module of the compressive sensing receiver, and then the dechirp module accomplishes the mixing of the reference signal with the original echoes. Unlike the traditional spotlight SAR receiver, the deskew module must be embedded in the dechirp processing, thus the receiver via compressive sensing induces some complexity compared with the traditional spotlight SAR receiver. Through dechirp processing, the echoes are randomly sampled and are quantified as a prescriptive data frame for downloading in the compressive sensing quantization (CSQ) module.

Figure 4 shows the procedure for data acquisition and processing based on compressive sensing. We can see that the radar platform transmits a few data bits by random sampling to the ground system in data processing, and the recovery of the original echoes is accomplished by using this land-based system. The reconstructed echoes can be used for real-time imaging concentrated on the hotspot areas.

Two approaches of random sampling are shown in Figure 5. The first one is digital random sampling. After dechirp sampling, the analog echoes are sampled to produce the digital signals by an analog-to-digital (A/D) converter, and then the data are randomly sampled. We often use the Gaussian random matrix to measure the digital signals. Direct random sampling of the analog echoes provides a the second

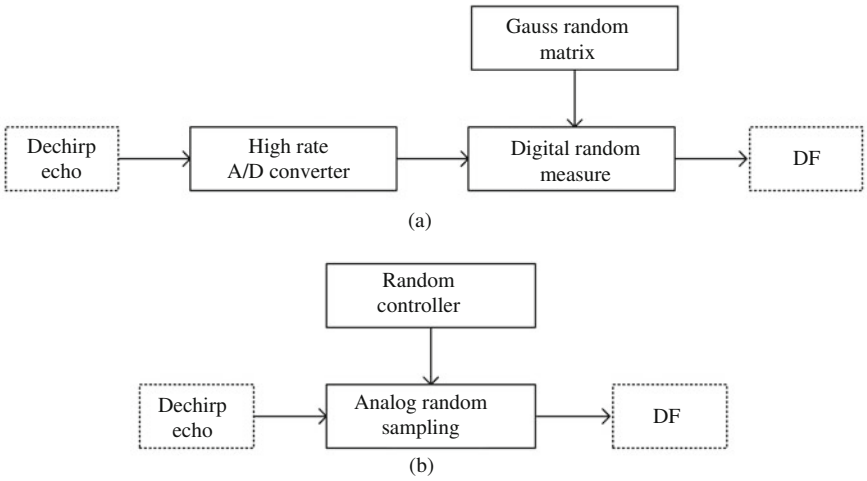

Figure 5 Digital and analog approaches for CSQ. (a) Digital random sampling; (b) analog random sampling.

approach, where, after random sampling, the signals are converted into the digital frame. Both advantages and some deficiencies are in these random sampling approaches. For digital random sampling, a small cost is associated with the construction of the measurement matrix. We can preset the Gaussian random matrix in the storage part of the CSQ module to measure the digital signals with the same distribution in each azimuth direction. The analog random sampling approach has high requirements with regard to the controlling A/D converter's ability to randomly switch on and off in each azimuth direction, however, although the random controller causes high sampling complexity, it avoids the need to pre-store the measurement matrix. In [18], a random sampling approach based on several FIR filters is presented, i.e. acting as a random filter. It sets the weights of the FIR filters to be independent and identically distributed random variables, and under-sampling the original signals to obtain the compressed data.

3.3 Analysis of the rationality of the dechirp basis

To maintain the convergence of the reconstruction algorithm, the measurement matrix and the sparse basis must satisfy the RIP, and the Gaussian random matrix set in random sampling can meet the equipollence form of RIP. In conclusion, the sparse basis is irrelative to this measurement matrix. The echoes can be considered to be a linear combination on the sparse basis, as shown in Eqs. (9) and (12), after dechirp processing in the radar receiver. The dimensions of the sparse basis are limited by the number of targets K and the length of the echoes N.

We define the correlative coefficient of the sparse basis as $\mu = |\langle\psi_i, \psi_j\rangle|$, which is an index of the rationality of the dechirp basis, and when $t_k = 2(R - R_{\text{ref}})/c$, Eq. (7) can be rewritten as

$$S_{\text{IF}}(t') = A\text{rect}\left(\frac{t' - f_c/K_r - t_k}{T}\right)\text{e}^{-\text{j}2\pi K_r t_k t'}, \tag{13}$$

if $t_i < t_j$, and there is an intersection between a pair of rectangular windows, then the μ value of the ith and jth subsets in $\boldsymbol{\Psi}$ is given as

$$\mu = |\langle\psi_i, \psi_j\rangle| = \left|\int_{-\frac{T}{2}+t_i+\frac{f_c}{K_r}}^{\frac{T}{2}+t_j+\frac{f_c}{K_r}} \text{e}^{-\text{j}2\pi K_r(t_j - t_i)t}\text{d}t\right|. \tag{14}$$

The approximate result of Eq. (14) is

$$\mu \leqslant \frac{cN}{4\pi K_r R_{\text{ref}}}, \tag{15}$$

and when the maximum correlative coefficient tends towards zero, the sparse basis can satisfy the orthogonality with the determinate conditions.

Table 1 Imaging parameters in range direction

Carrier frequency	1.5 GHz
Signal bandwidth	150 MHz
Pulse time width	1.3 μs
Range signal length N_r	1024
Random sampling number M	102
Target numbers, sparse-level K	8

4 Simulation results

4.1 Radar imaging in range direction

A one-dimensional observation scene in the range direction with K targets is simulated for imaging, and the system parameters for the simulations are shown in Table 1. We use S to represent the original echoes after dechirp processing, and the I and Q components are sampled with the preset measurement matrix. In detail, the echoes of a certain target contain both real parts and imaginary parts, and these data are projected into the low-dimensions with the same Gaussian random matrix. The MP algorithm uses the dechirp basis and the Gaussian random matrix to extract the location and backscatter coefficient information, and the dechirp basis is combined with these backscatter information to reconstruct S.

Calculating the maximum correlative coefficient according to Eq. (15) using the parameters given in Table 1, we obtain a result of

$$\mu_{\mathrm{MAX}} = 7.225 \times 10^{-8}. \tag{16}$$

We define the compression ratio as

$$D = \lfloor N/M \rfloor, \tag{17}$$

where the length of the signal S is N =1024, and the random sampling number is M =102, so that the compression ratio is approximately 10, through random sampling , which means that the amount of data of signal S to be reserved is merely 10%. We use $\hat{S}$ to represent the signal that was reconstructed by the MP algorithm. Figure 6 shows a comparison of the real and imaginary parts of the signal S and $\hat{S}$. Figure 7 shows the error curve of the real parts of signals S and $\hat{S}$, which is the amplitude error of the corresponding points in the time domain between S and $\hat{S}$. As shown in Figure 7, the amplitude error is comparatively enhanced at the beginning and the end of the pulse duration time.

The error curve is merely an intuitive comparison between the amplitudes of the corresponding points of signals S and $\hat{S}$. We thus define the relative error as an index applied to analyze the quality of the reconstructed signal $\hat{S}$.

$$\mathrm{error} = \frac{\|\hat{S} - S\|_2}{\|S\|_2}. \tag{18}$$

The expression for the relative error is given in Eq. (18), where $||.||_2$ is the l_2 norm. In subsequent simulations, we will use the error curve and the relative error to review the effects of the measurement dimensions and the signal-to-noise ratio (SNR) on the precision of signal reconstruction. The measurement dimensions depend on the random sampling number M, and the appropriate value of M is highly significant for both the data compression and the precision of the signal reconstruction. Figure 8 shows the curve of the measurement dimension M, which affects the precision of the reconstruction, as seen in this figure, when $M \geqslant 12K$, and K is sparse-level, the error curve begins to fluctuate with a low amplitude, and the relative error curve still indicates the same trend. It is notable that the reconstruction error is represented by this up-and-down trend due to the randomness of the measurement matrix. In practical applications, a fixed measurement matrix can be used to improve the reconstruction speed, and to ensure that the randomness of the measurements has little effect on the reconstruction error.

In practice, radar echoes contain noise, for example, the system thermal noise in the received echoes cannot be ignored. Under noise interference conditions, we simulate the effects of the variation in SNR

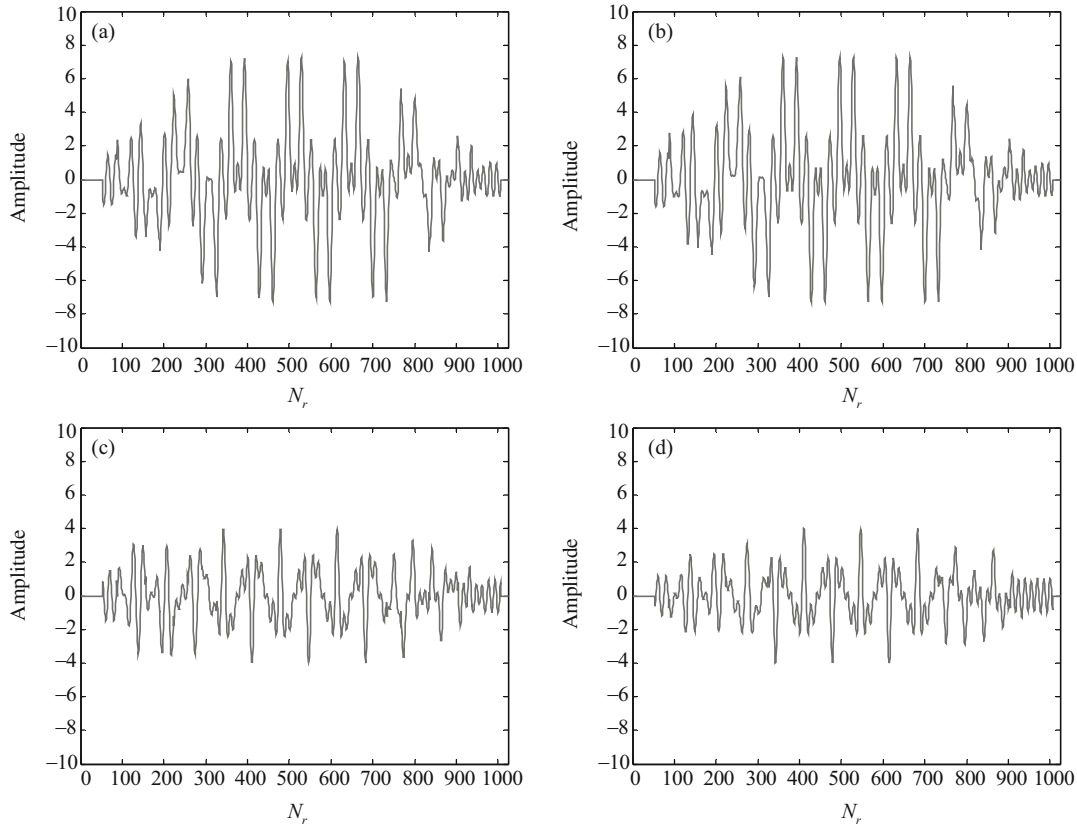

Figure 6 Comparison of signals S and $\hat{S}$. (a) The real part of signal S; (b) the real part of signal $\hat{S}$; (c) the imaginary part of signal S; (d) the imaginary part of signal $\hat{S}$.

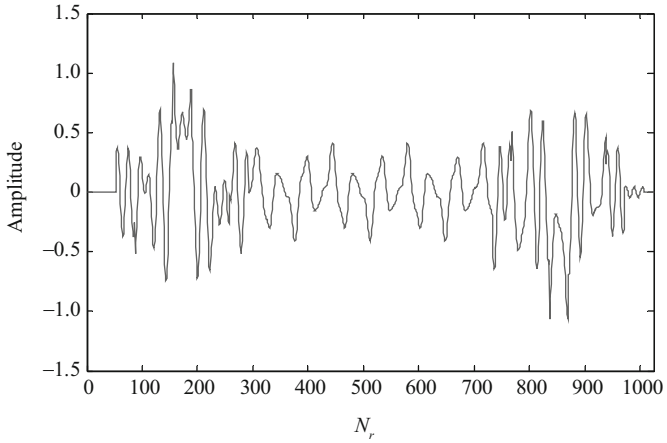

Figure 7 Error curve of real parts in signals S and $\hat{S}$.

values on the reconstruction error with a fixed value of M. The results are shown in Figure 9, where the fluctuation of the error curve tends to stabilize when the SNR is $\geqslant$ 30 dB, while the relative error maintains a consistent trend.

Finally, we use the original echoes and the reconstructed echoes for imaging. Figure 10 shows the imaging results in the range direction. Although a great deal of the original data is discarded, the simulation results verify that 10% of the original data is still sufficient to achieve high quality imaging results, and the dechirp basis can be used to sparsely disassemble the original echoes and reconstruct the echoes with high probability.

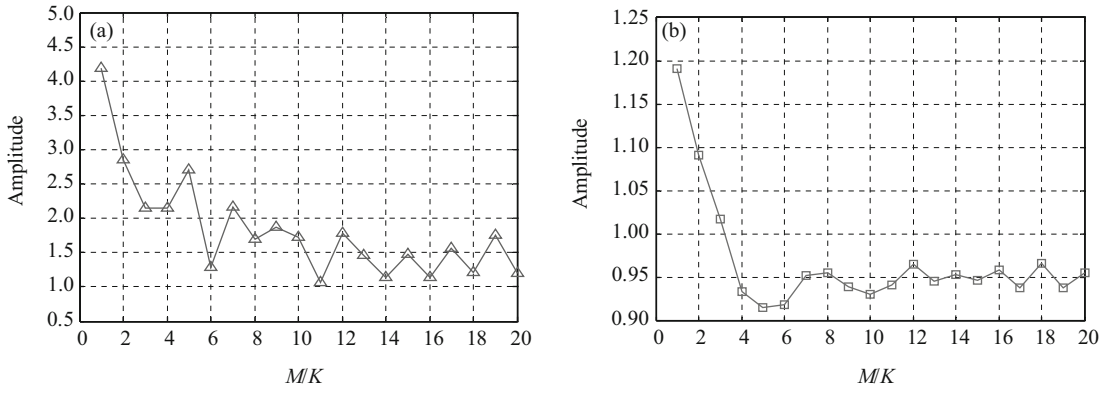

Figure 8 The effects of the measurement dimension M on the reconstruction precision. (a) Amplitude error curve; (b) relative error curve.

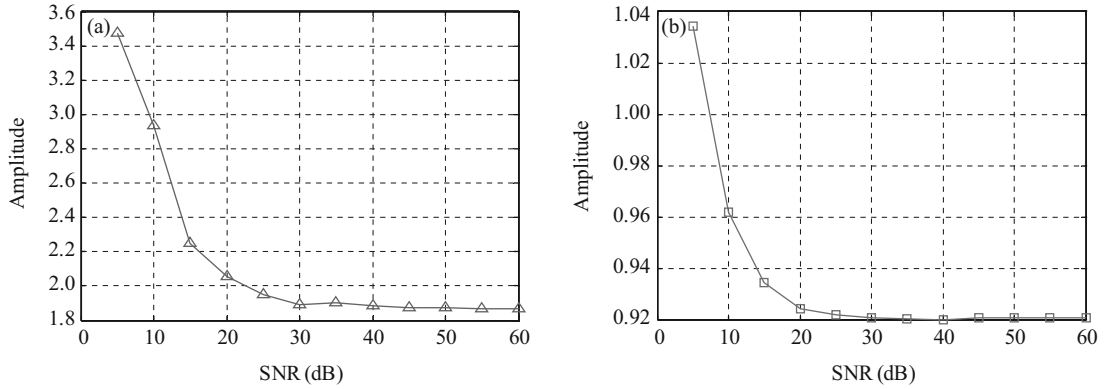

Figure 9 The effect of SNR on the reconstruction precision for M=100. (a) Amplitude error curve; (b) relative error curve.

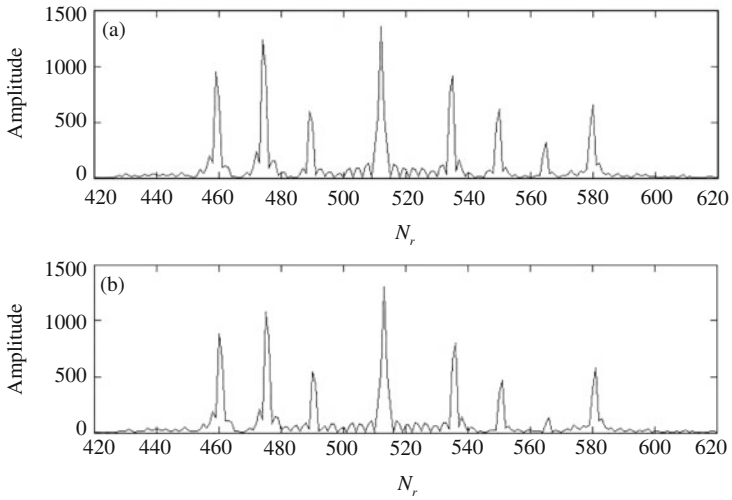

Figure 10 The imaging results for the original echoes S and the reconstructed echoes $\hat{S}$. (a) Imaging result of origin echo; (b) imaging result of reconstructed echo.

4.2 Radar imaging with two-dimensional signals

The echoes of spotlight SAR are two-dimensional signals. The radar platform receives the chirp echoes in each azimuth direction when the platform moves along the track direction, and the echoes of the observed

Table 2 Imaging parameters for point target

Carrier frequency	9.4 GHz
Signal bandwidth	150 MHz
Chirp pulse duration time	10 μs
PRF	400 Hz
Platform velocity	250 m/s
Signal length N_a, N_r	1024

scene are stored in a two-dimensional matrix memorizer in a time sequence. In the first instance, we set a fixed reference range, generally choosing the center point of the observed scene as the reference target, to dechirp the echoes in each azimuth direction, the simulation parameters selected are shown in Table 2. The dechirped echoes are then predestined for sampling with the fixed random measurement matrix. The echoes are randomly sampled after dechirp processing to construct the measurement vectors, and the MP algorithm uses these vectors and the dechirp basis to extract the backscattering information. Note that the distance between the target and the platform varies along the azimuth direction, so that the position information of the target is undetermined, and thus it is essential to reconstruct the echoes using the dechirp basis in each azimuth direction to recover the scene.

Spotlight SAR often uses the polar format algorithm [19,20] (PFA) for imaging. Because the reference range is imported by dechirp processing, it overcomes the range cell migration in image processing. The PFA accomplishes pulse compression in the range direction and in the azimuth direction through two-dimensional Fourier transform, but the necessary range and azimuth interpolation required to reset the data format is taken into account for a two-dimensional fast Fourier transform.

A comparison of the imaging results achieved using PFA with the original echoes and with the reconstructed echoes is shown in Figure 11. In this simulation, there is a scattering points array positioned in the observed scene. The top charts show the imaging results for the original echoes and 10% of the data randomly sampled from the original echoes. The bottom charts in Figure 11 represent the details of the center point of the observed scene. To investigate the performance of the aforementioned signal processing via compressive sensing, several imaging quality estimation terms are evaluated and Figures 12 and 13 show the results of imaging quality estimation for the point target in the charts of Figure 11. As represented in Figure 13, the high imaging quality is maintained in the echoes reconstructed by only 10% of the original data. Table 3 lists some indexes for imaging quality estimation, the values listed for the corresponding indexes are very approximate.

Indicating that imaging with only 10% of the original echoes can produce highly accurate results, but the reconstruction processing has a large calculation load. For instance, the simulation shown in Figure 11, the simulation hardware used 4 GB of memory, and an Intel Core i3 model CPU with a main frequency of 3.07 GHz, which meant that it needed 728.270156 s for imaging with data reconstructed using 10% of the original echoes, while imaging with the original echoes costs only 10.219449 s, meaning that the calculation time for the former is approximately 70 times that of the latter, apparently, a highly effective reconstruction algorithm is a critical problem for compressive sensing application to radar signal processing.

In real-time observation, the sparse-level K of the observed scene is generally undiscovered. To solve the problem of sparse basis construction with an indeterminate K, we propose to construct a complete sparse basis by partitioning of the observation grids, which decreases the requirements for prior information about the sparse-level K. Once the size of the observed scene is determined, by dividing the distances in the range direction and the azimuth direction by the same resolution cell, the scattering points should be placed on the nodes of observation grids. On the assumption that each node contains a single scattering point, the complete sparse basis can be designed using the locations of nodes. Obviously the minuteness grids can improve the completeness of the sparse basis.

Figure 14 shows an imaging simulation of a warship target under noise-free conditions. Ignoring the sea background, the Kiev aircraft carrier used as a target pattern is extracted in an optical image, and the original echoes of the warship target are simulated for dechirp processing. The warship is an extended

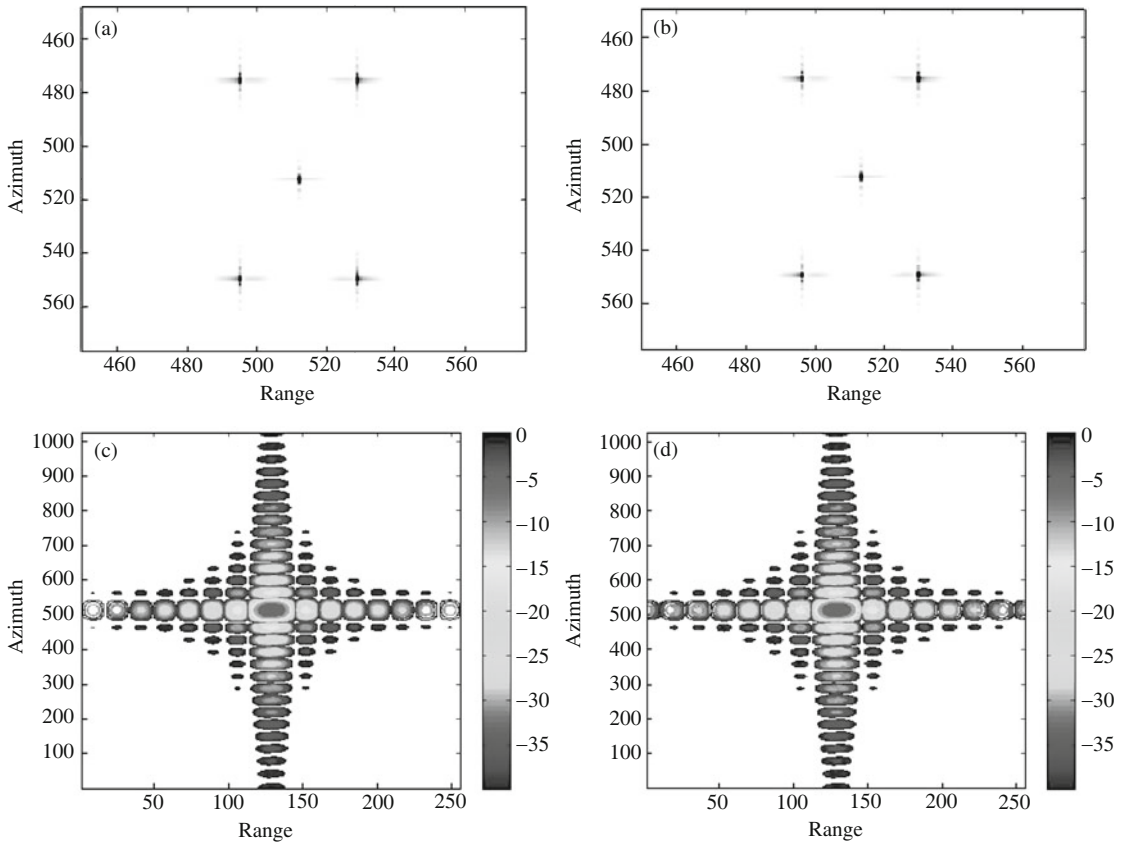

Figure 11 Comparison of imaging results. (a) Imaging result using original echoes; (b) imaging result for reconstructed echoes, 10% data; (c) the center point shown in (a); (d) the center point shown in (b).

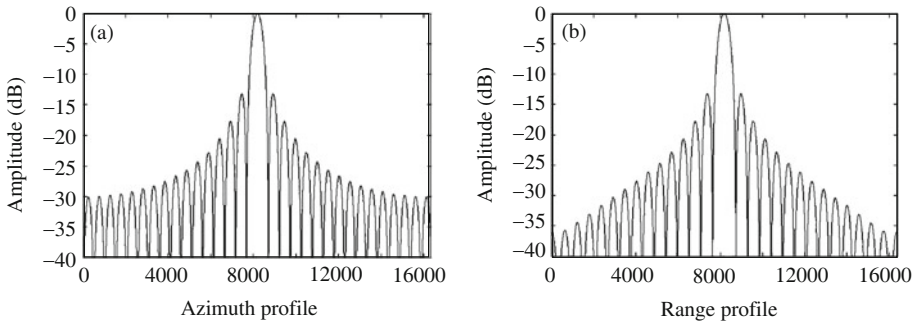

Figure 12 Cross-sections of the center point in Figure 11(a). (a) The azimuth cross-section; (b) the range cross-section.

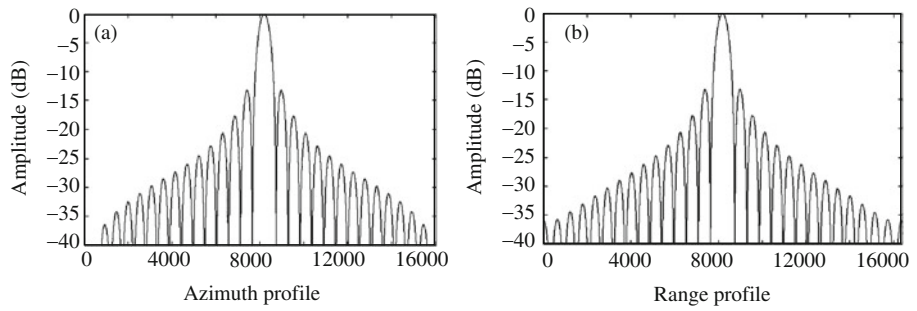

Figure 13 Cross-sections of the center point in Figure 11(b). (a) The azimuth cross-section; (b) the range cross-section.

Table 3 Imaging quality estimation for the center point in observed scene

Parameters	Imaging with reconstructed echoes		Imaging with original echoes	
	Azimuth	Range	Azimuth	Range
Resolution (m)	0.578	1.070	0.533	0.963
PSLR (dB)	−13.231	−13.426	−13.233	−13.239
ISLR (dB)	−9.982	−10.081	−9.698	−10.050

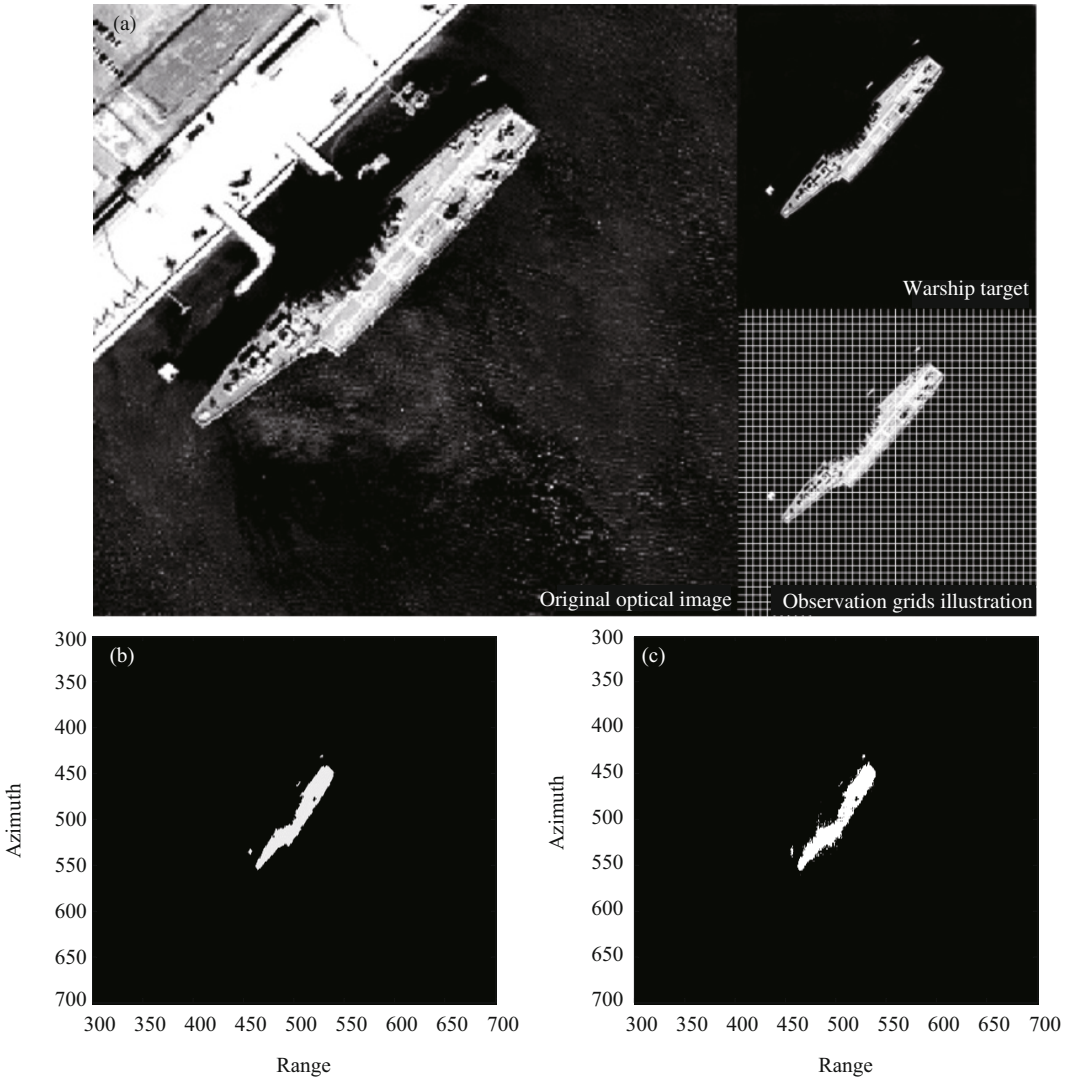

Figure 14 Imaging simulation of a warship target. (a) Optical image of the warship target; (b) imaging result of spotlight SAR from the original data; (c) imaging results of spotlight SAR based on compressive sensing with 10% of the original data.

target on a sea background, but the observed scene is spatially sparse, and thus dividing the observed scene with observation grids to construct the complete sparse basis is the first step in the imaging process, followed by the collection of 10% of the data of the original echoes by random sampling to compose the measurement vector in each azimuth direction. The complete sparse basis and the measurement vector are imported into the MP algorithm to obtain the scattering points information. Finally, using the backscatter and the complete sparse basis to reconstruct the original echoes, we use the PFA to obtain the spotlight SAR image. The imaging result using the original echoes is shown in the bottom left chart of Figure 14, while in the bottom right chart of Figure 14, 10% of the data of the original echoes is used for imaging, and Table 4 lists the simulation parameters.

Table 4 Imaging parameters for warship target

Carrier frequency	9 GHz
Signal bandwidth	200 MHz
Chirp pulse duration time	10 μs
PRF	600 Hz
Platform velocity	250 m/s

In this simulation, we intentionally reserved three scattering targets near the warship in the optical image, but discarding 90% of the data of the original echoes cannot induce the absence of the small scattering targets. The imaging results for the warship target indicate that the sparse basis is applicable for observation of target scenes with rather excessive scattering points, because the non-sparse numbers of scattering points cannot induce an unsuccessful reconstruction. However, as shown in Figure 14, the edge of the warship is not smooth enough in the imaging result based on compressive sensing, which demonstrates that the locations of the scattering points deviate from a regular pattern. The close-set scattering points therefore lower the quality of the imaging result, whereas, the signal processing method for spotlight SAR based on compressive sensing presented in this paper is not restricted by the complex observation scene. It reduces the requirements for sparse-level K in observed scenes and extends the application of compressive sensing in radar signal processing.

5 Conclusion

This paper introduces a data acquisition and processing approach based on compressive sensing for spotlight SAR. The novel processing mechanism uses a reduced number of original echoes after dechirp processing to reconstruct the target scene, and it overcomes the restrictions on the sparseness levels of observed scene. A non-sparse scene cannot induce an unsuccessful reconstruction, however, the observation area of spotlight SAR is limited, we must extend the applicability of radar signal processing via compressive sensing for spotlight SAR, e.g. using the mosaic mode [21] to achieve a wide observation area, combining this mode, the scan mode in range direction and the spotlight mode in azimuth direction, with the radar signal processing method presented in this paper will be part of our continuing research. Compressive sensing aims to use a reduced data to reconstruct the original signal, but this signal sampling and recovery method discards the partial information of the original signal and consequently increases the reconstruction calculation loads. The design of a rapid and effective reconstruction algorithm and the appropriate compression ratio are thus crucial for real-time imaging applications.

Acknowledgements

This work was supported by National Key Basic Research Project (Grant No. 2010CB731902).

References

1 Carrara W G, Goodman R S, Majewski R M. Spotlight Synthetic Aperture Radar: Signal Processing Algorithms. Boston: Artech House, 1995
2 Kashin B. The widths of certain finite dimensional sets and classes of smooth functions. Izv Akad Nauk SSSR Ser Mat, 1977, 41: 334–351
3 Baraniuk R, Steeghs P. Compressive radar imaging, In: IEEE Radar Conference, Boston, 2007. 128–133
4 Herman M A, Strohmer T. High-resolution radar via compressed sensing. IEEE Trans Signal Process, 2009, 57: 2275–2284
5 Tello Alonso M, Lopez-Dekker P, Mallorqui J J. A novel strategy for radar imaging based on compressive sensing. IEEE International Geoscience & Remote Sensing Symposium (IGARSS), Boston, 2008. 213–216
6 Ender J H G. On compressive sensing applied to radar. Signal Process, 2010, 90: 1402–1414
7 Caputi W J. Stretch: A time-transformation technique. IEEE Trans Aerosp Electron Syst, 1971, 7: 269–278

8 Wehner D R. High Resolution Radar. Norwood: Artech House, 1987
9 Giorgio F, Ricacardo L. Synthetic Aperture Radar Processing. Boca Raton: CRC Press, 1999
10 Donoho D. Compressed sensing. IEEE Trans Inf Theory, 2006, 52: 1289–1306
11 Candes E J. Compressive sampling. In: Proceedings of the International Congress of Mathematicians, Madrid, 2006. 1433–1452
12 Candes E J, Romberg J, Tao T. Robust uncertainty principles: Exact signal reconstruction from highly incomplete frequency information. IEEE Trans Inf Theory, 2006, 52: 489–509
13 Blumensath T, Davies M E. Gradient pursuits. IEEE Trans Signal Process, 2008, 56: 2370–2382
14 Davis G, Mallat S, Avellaneda M. Greedy adaptive approximation. J Constr Approx, 1997, 12: 57–98
15 Donoho D, Elad M, Temlyakov V. Stable recovery of sparse overcomplete representations in the presence of noise. IEEE Trans Inf Theory, 2006, 52: 6–18
16 Mallat S G, Zhang Z F. Matching pursuits with time-frequency dictionaries. IEEE Trans Signal Process, 1993, 41: 3397–3415
17 Tropp J A, Gilbert A C. Signal recovery from random measurement via orthogonal matching pursuit. IEEE Trans Inf Theory, 2007, 53: 4655–4666
18 Tropp J A, Wakin M B, Duarte M F, et al. Random filters for compressive sampling and reconstruction. In: IEEE International Conference on Acoustics, Speech, Signal Processing (ICASSP), Kyoto, 2006
19 Brookner E. Synthetic Aperture Radar Spotlight Mapper. Dedham: Artech House, 1977
20 Jakowatz C V, Wahl D E, Eichel P H, et al. Spotlight-Mode Synthetic Aperture Radar: A Signal Processing Approach. Boston: Kluwer Academic Publisher, 1996
21 Naftely N, Levy-Nathansohn R. Overview of the TECSAR satellite hardware and mosaic mode. IEEE Geosci Remote Sens Lett, 2008, 5: 423–426